CONTINUING EDUCATION PROGRAM: FOCUS...

Radionecrosis of malignant glioma and cerebral metastasis: A diagnostic challenge in MRI

A. Raimbault[a], X. Cazals[a], M.-A. Lauvin[a],
C. Destrieux[b], S. Chapet[c], J.-P. Cottier[a],*

[a] General Radiology - Diagnostic and Therapeutic Neuroradiology, Bretonneau Hospital, 2, boulevard Tonnellé, 37044 Tours cedex, France
[b] Department of Neurosurgery, Bretonneau Hospital, Tours University Hospitals, 2, boulevard Tonnellé, 37044 Tours cedex, France
[c] Department of radiotherapy, Bretonneau Hospital, Tours University Hospitals, 2, boulevard Tonnellé, 37044 Tours cedex, France

KEYWORDS
Radionecrosis;
Radiotherapy;
Malignant glioma;
Brain metastasis;
Tumor recurrence

Abstract   Detecting a new area of contrast-enhancement at MRI after irradiation of malignant brain tumor arises the problem of differential diagnosis between tumor recurrence and radiation necrosis induced by the treatment. The challenge for imaging is to distinguish the two diagnoses given: the prognostic and therapeutic issues. Various criteria have been proposed in the literature based on morphological, functional or metabolic MRI. The purpose of this study was to perform an analysis of these tools to identify MRI best criteria to differentiate radiation necrosis lesions from malignant gliomas and brain metastases recurrence. For gliomas, the morphology of the contrast-enhancement cannot guide the diagnosis and the use of perfusion techniques and spectroscopy (multivoxels if possible) are necessary. In the follow-up of metastasis, a transient increase and moderate lesion volume is possible with a good prognosis. Morphological characteristics (volume ratio T2/T1Gd) and perfusion analysis provide valuable tools for approaching the diagnosis of radionecrosis.

Malignant glial tumors and metastases currently account for more than half of brain tumors (20 and 33% respectively) [1,2] and are increasing in incidence. Radiotherapy (RT) is an important component of the treatment options for these tumors whether used alone or postoperatively. Conventional RT is given for glial tumors whereas the choice of type of irradiation (whole brain or stereotactic for cerebral metastases) depends on the number of lesions (stereotaxis is possible when there are no more than 3 to 5 secondary lesions), and on their size.

* Corresponding author.
  E-mail address: cottier@med.univ-tours.fr (J.-P. Cottier).

This radiotherapy, which has been shown to be effective (radiology control of metastases in 90% of cases with stereotactic RT and a significant improvement of survival of patients receiving radiochemotherapy with temozolomide (Temodal®) following excision surgery for high-grade gliomas) although may cause severe symptomatic necrotic and inflammatory effects and/or effects responsible for worrying appearances. The irradiation related inflammatory and necrotic effect is then responsible for contrast-enhancement, edema and a space-occupying lesion, which is very difficult to distinguish from recurrence or continued active disease.

The incidence of pronounced radio-induced lesions has been estimated depending on the series as between 3 and 24% [3,4] for glioblastomas and approximately 25% for irradiated metastases [5]. This figure, however, is rising because of successive irradiation achieved by the use of stereotactic RT and is underestimated (it is seen concomitantly with recurrences and is involved in the pseudoprogression seen with temozolomide).

During post-irradiation follow-up, the development (or increase) in contrast-enhancement or an increase in size of volume of the initial lesion therefore raises the question of whether the disease has progressed despite treatment, or whether temporary irradiation-induced necrosis has developed. The difficult role of the expert radiological assessment is to attempt to make this differential diagnosis in order to adapt the subsequent treatment plan or radiological monitoring. Several studies (with conventional imaging and particularly functional and metabolic imaging techniques) have attempted to propose radiological signs or values, which are in favor of necrosis or tumor recurrence, although their sensitivities and specificities vary and are occasionally contradictory. There is at present no consensus about these radiological appearances [6,7]. In addition, the results of these studies are difficult to incorporate into everyday's practice because of variations in the imaging techniques used, the heterogeneous populations studied (malignant gliomas and metastases) and types of irradiation (whole brain RT, hypo- or normofractionation or stereotactic RT).

The aim of this report is to analyze the current morphological, functional and metabolic imaging tools from a literature review in order to identify the best criteria to distinguish radionecrosis lesions from a tumor recurrence after the treatment of malignant gliomas and cerebral metastases.

Cerebral radionecrosis: general information

Pathological anatomy

Although the mechanism of radio-induced lesions is not entirely understood, it is accepted that the initial damage is vascular, and it is followed by glial and neuronal effects. This is combined with changes in the enzyme system and immunological mechanisms. These lesions are seen a few months to a few years after radiotherapy has finished and are generally irreversible and progressive.

In the acute phase, vasodilatation occurs with increased capillary permeability resulting in vasogenic edema [3,8].

Thickening of the vascular walls then develops through hyalinization, fibrinoid necrosis of both the vascular wall and endoluminal thrombi leading to infarction and tissue necrosis [9]. The extension and confluence of necrotic effects produce a serpiginous or geographical appearance in necrotic parenchyma [3]. Analysis of tissue from radionecrosis lesions has shown an absence of tissue plasminogen activator and excess plasminogen urokinase activator. This imbalance may contribute to the secondary cytotoxic edema, which leads to tissue necrosis. Vascular endothelial growth factor (VGEF) has also recently been implicated [10]: perinecrotic tissue astrocytes are VEGF positive, contributing to the local proliferation of endothelial cells. Chronically, vascular architectural changes, which may produce telangiectasiae, may occur.

Oligodendrocytes are extremely radiation sensitive and their destruction results in the demyelination lesions seen around the necrotic areas [3,11]. The parenchymal lesions mostly affect the white matter (WM) and underlying laminar layer of the cortex, whereas the superficial cortex is relatively spared [12]. Immunologically, a true immune reaction is believed to develop against the host. In the late phase, apart from gliosis and parenchymal atrophy, cysts and dystrophic calcifications may develop.

It should be noted that post-irradiation lesions are always present to variable degrees in histological examinations of excised tissue and which enhance on imaging in the irradiated area accounting for between 30 and 65% of the tissue removed in recurrences of glioblastomas [13,14].

Risk factors

The factors predisposing to radionecrosis following conventional RT are the total irradiation dose, the size of the volume irradiated [15,16], a small number of fractions [4], the staggering of the treatment over time, a combination of chemotherapy, length of survival and patient age (young patients) at the time of the irradiation. The most important risk factor is the total irradiation dose received. The incidence of radiation necrosis doubles and quadruples when the doses exceed 62 Gy and 78 Gy respectively.

In stereotactic RT, the specific risk factors are the volume irradiated at the 12 Gy dose (over 8 cc), previous irradiation and male sex [17,18].

The chemotherapies which promote the development of radio-induced lesions are cisplatin and carboplatin, doxorubicin, methotrexate and temozolomide [17,19].

Time to onset

The average time between irradiation and clinical or radiological suspicion of radionecrosis in patients who have received a total brain dose of > 50 Gy is one year, although cases have been reported from a few months up to several years after treatment [20]. RT causes the lesions described in the literature under the term pseudoprogression in the initial weeks or months after RT for a high-grade glioma combined with chemotherapy.

Early radionecrosis and pseudoprogression

The current reference treatment protocol for glioblastomas (Stupp et al. [21]) includes optimal excision of the tumor

followed by conventional focused beam radiotherapy and concomitant chemotherapy and then adjuvant chemotherapy with temozolomide. A large increase in the size of contrast-enhancement is seen in the weeks or months after radiotherapy finishes as a result of this treatment and mimics actual tumor progression [22]. This phase, during which appearances exacerbate (''pseudoprogression''), is reported in 20 to 30% of cases and is followed by a secondary improvement or stabilization without additional treatment [23]. Patients with methylation of the gene coding for a repair enzyme for chemotherapy-induced lesions, O-6-methylguanine-DNA-methyltransferase (MGMT), develop this reaction more commonly [23]. The reaction is subacute and asymptomatic in most patients (70%). Its features (increase or development of contrast-enhancement occurring early and falling over time) are also seen in radiotherapy without temozolomide although is more common and occurs earlier when temozolomide is used in association. Effective radiotherapy is believed to cause a breach in the blood-brain barrier (BBB) facilitating the passage of the drug and resulting in an increase in its activity. In early radionecrosis, gliosis combined with inflammatory changes are also described in tissues in the absence of viable tumor cells. Early radionecrosis may therefore be a variant of pseudoprogression and some authors have proposed that the concept of treatment-induced necrosis and its radiological features should be included in the term pseudoprogression and replace the former term, early radionecrosis [24].

Methods of making the final diagnosis

The final diagnosis of radionecrosis may be made from histological findings or from clinical and radiological follow-up:
- histological findings obtained from excision of a symptomatic lesion or biopsy (although this raises the problem of how representative the fragment is);
- clinical and radiological outcome, which requires observation periods depending on the studies of between 4 and 9 months [5,8]. Lesions which regress or remain stable on follow-up MRI during hisperiod without additional oncology treatment are deemed to be post-irradiation damage. Those which increase progressively in size, often with concomitant clinical deterioration, are interpreted as recurrence of tumor.

Magnetic resonance imaging of radionecrosis

Whilst the underlying histological changes in radionecrosis are consistent in both situations, MRI findings (morphological, functional and metabolic) and the diagnostic problems these arias are very different after treatment for a malignant glioma or metastasis.

After treatment of a malignant glioma

Conventional imaging

The classical appearances are those of a mass which enhances, with a central necrotic area (Fig. 1). Contrast-enhancement reflects breach of the BBB secondary to the endothelial irradiation-induced damage. The lesions usually

occur at the site of the maximum irradiation dose, i.e. in the immediate vicinity of the tumor site and around the excision cavity. These are predominantly in the white matter which contains perivascular coagulative necrosis. The white matter is particularly vulnerable to the secondary ischemic consequences of post-irradiation vasculopathy [25]. The deep white matter has a relatively poor blood supply from the long spinal arteries and has no collateral arterial supply. The white matter arcuate fibers which also receive cortical arterial supply are more resistant to radionecrosis and are therefore usually affected later in the disease process.

The type of contrast uptake varies greatly. Enhancement may be nodular, linear or curvilinear [4], heterogeneous and annular producing ''cut-green pepper'' (Fig. 1), ''soap bubbles'' or ''gruyere'' cheese appearances [3,26]. Blurred plumed boundaries appear to suggest radionecrosis compared to the nodular boundaries with clear edges in tumor recurrence [27]. If the cortex is affected, contrast uptake may be gyriform [3].

Whilst these effects are predominantly seen in the initial tumor sites, single or multifocal post-irradiation contrast-enhancement may also be present remote to the tumor. This was found several centimeters from the initial site in 14 of Kumar et al.'s [3] series of 26 cases of radionecrosis affected the corpus callosum in 6 patients, the contralateral hemisphere in 8 patients, the subependymal regions in 8 patients and the posterior fossa in 5 patients.

Hypointensities indicative of hemorrhagic changes are often seen on T2-weighted echogradient images. These were reported in 53% of cases of radionecrosis by Chan et al. using the conventional T2* sequence [28] and in 80% of cases of radionecrosis using magnetic susceptibility imaging by Zeng el al [29].

The space-occupying effect is typically very small for the size of lesion although the reactive vasogenic edema which accompanies it can however be extensive and cause a significant space-occupying effect. The immediate change in contrast-enhancement varies depending on the dynamic pathophysiological process in radionecrosis lesions. In cases of possible radionecrosis, overan observation period over a few months, some lesions continue to enlarge with a transient increase in the cytotoxic edema, some lesions remain stable before regressing and others regress from the start (Fig. 2). Early surgery may be required for symptomatic
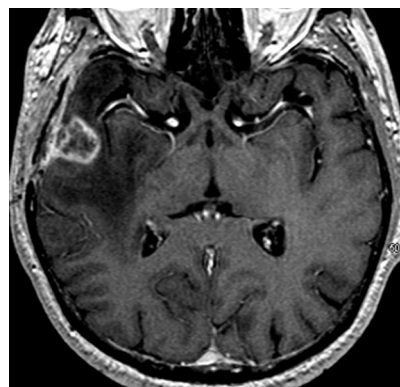

Figure 1. Right temporal radionecrosis. Nodular contrast-enhancement with irregular boundaries containing fine internal reticulation giving it a ''cut-green pepper'' appearance.
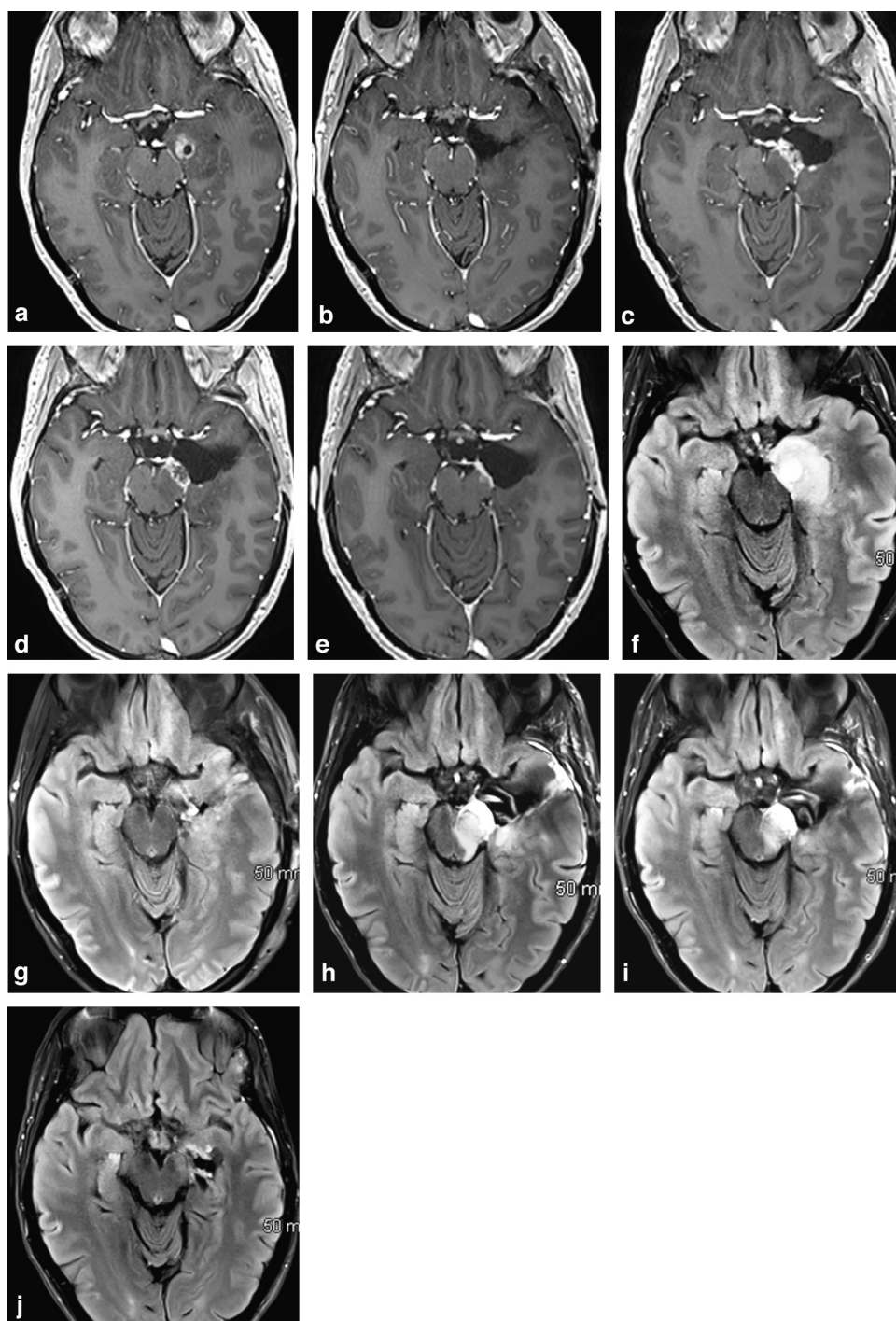
Figure 2.   Changes inradionecrosis lesions. T1-weighted axial images after gadolinium (a-e) and T2 FLAIR (f-j). High-grade left medial temporal glial lesion (a) treated by surgery (complete excision), then RT and temodal chemotherapy (b: repeat MRI 3 months after surgery). Development of medial temporal contrast and mesencephalic contrast-enhancement associated with perilesional edema on the repeat MRIat 6 months (c,h). On the repeat MRI performed 3 months later (d,i), there is an increase in the necrotic appearances of the lesion with slight regression of the T2-weighted hyperintensity. Three months later the contrast-enhancement has disappeared and the perilesional edema has melted away (e,j).

active expansile lesions to reduce the space-occupying effect and provide an unequivocal diagnosis.

Overall, the morphological features of radionecrosis lesions are very similar to those of a recurrent tumor: type of contrast-enhancement, site (both in the tumor site and remote) and possible transient deterioration [3]. According to Mullins et al. [26], some combinations of contrast-enhancement remote to the initial tumor site argue more in favor of tumor recurrence: involvement of the corpus callosum associated with multiple enhancement sites, and of the corpus callosum associated with subependymal contrast-enhancement (Fig. 3).
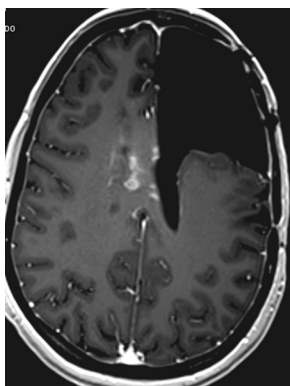
Figure 3. Recurrence of glioblastoma. T1-weighted axial image after gadolinium. Appearance of contrast-medium in the corpus callosum and the walls of the postoperative cavity.

Diffusion-weighted imaging

The apparent diffusion coefficient values (ADC) proposed to distinguish recurrence from radionecrosis in the literature are contradictory (Table 1).

Several studies have shown a significantly lower ADC in tumor recurrence compared to radionecrosis [8,30]. Histologically, tumor recurrence contains areas of viable tumor cells with pleimorphic nuclei and a dense network of cytoplasmic processes, whereas radiation-induced tissue necrosis is paucicellular with increased water in the interstitial spaces. According to Hein et al. [30], the ADC ratio (rADC or mean ADC of the contrast-enhancing area/mean ADC of the same area in the contralateral hemisphere) is more discriminatory than absolute ADC values, with a significantly higher rADC in radionecrosis (rADC = 1.82) compared to tumor recurrence (rADC = 1.43). Asao et al. [8] assessed mean and maximum ADC values in these areas of heterogeneous structure enhancement. All three values were lower in tumor recurrences although no significant difference was found except for the maximum ADC (1.68. 10^{-3} mm/s^2 mean compared to 2.3 $\times 10^{-3}$ mm/s^2 for radionecrosis).

Unlike previous studies, Sundgren et al. [31] found significantly higher mean ADC values in the recurrence group (1.27×10^{-3} mm/s^2) than in the radionecrosis group of patients (1.12×10^{-3} mm/s^2) and no significant difference was found between the two groups in another study [32].

Whilst a low ADC is often seen in tumor recurrences because of high cellularity, ADC values may also be increased by microangiogenesis or necrotic effects. Conversely, fibrotic lesions and inflammatory effects involving macrophage and polynuclear cell influx [8] explain why the ADC is low in radionecrosis. Hemorrhagic changes with hemosiderin deposition can also lead to a reduced signal by a T2* or T2 dark-through effect [33].

It is also useful to study ADC values in the T2-weighted hyperintense area located outside of the contrast-enhancement (''perilesional edema''). The mean ADC in radionecrosis is not significantly different between the enhancing area and the neighboring area, whereas in tumor recurrences, the ADC is higher outside of the contrast-enhancement [30,34].

Diffusion tensor imaging

The anisotropic fraction (AF) is related to histological findings such as cellularity, vascularization and the structural organization of fibers. A relationship is seen between the fall in AF values and aggression of glial lesions [35]. In radionecrosis the fibers and normal cells are destroyed resulting in a reduced AF [36,37]. This is associated with an increase in mean diffusivity, also affecting the apparently normal white matter adjacent to the edema. [38].

Perfusion imaging

The vascular lesions in radionecrosis involve a combination of extensive fibrinoid necrosis and dilatation of blood vessels. Tumor recurrences are characterized by vascular proliferation with a high tumor vascular density. Histological examination has shown that tumor recurrences display significantly higher levels of neoangiogenesis than in radionecrosis [39,40], although the cerebral blood volume in tumor recurrences is significantly lower than in the initial glioblastoma [12,40]. Different ways of analyzing tissue perfusion are available: analysis of the first-pass gadolinium curve on T2*-weighted imaging, studying T1-weighted enhancement dynamics and analysis of arterial spin labeling (ASL).

Analysis of the first-pass gadolinium curve

This can provide information about the capillary microcirculation from measurement of various parameters: cerebral blood volume, amplitude of the signal deflection peak and percentage signal recovery.

Table 1 Diffusion values to distinguish radionecrosis from recurrence of a high-grade glial lesion.

	MF	Number of patients			Radionecrosis	Recurrence
		Total	RN	R		
[30]	1.5 T	18	6	12	ADCr = 1.82 + 0.07	ADCr = 1.43 + 0.11
[8]	1.5 T	20	12	8	ADC max = 2.3 + 0.73 10^{-3} mm/s^2	ADC max = 1.68 + 0.73 10^{-3} mm/s^2
[38]	1.5 T	28	12	16	ADC mean = 1.12 10^{-3} mm/s^2	ADC mean = 1.27 10^{-3} mm/s^2
					FA ratio = 0.89 + 0.15	FA ratio = 0.74 + 0.14
[57]	3 T	55	23	32	ADCmean = 1.39 10^{-3} mm/s^2	ADCmean = 1.2 10^{-3} mm/s^2
					ADCr = 1.69	ADCr = 1.42

MF: magnetic field; RN: radionecrosis; R: recurrence.

Because of neoangiogenesis the perfusion curves show a high relative cerebral blood volume (rCBV or the ratio between the blood volume in the lesion and the blood volume in the apparently healthy region of interest positioned in the contralateral white matter) in tumors compared to a low rCBV in radionecrosis (Table 2), (Figs. 4 and 5). The situation, however, is more complex because of tissue heterogeneity, breach of the blood-brain barrier and the presence of free radical damage inside and around the tumors [14,41] explaining the overlapping perfusion values.

The pilot study by Sugahara et al. [40] showed an rCBV cutoff of under 0.6 for radionecrosis and over 2.6 for tumor recurrence, with no clear diagnosis between these two values. More recently, Bobek-Billewics et al. [32] proposed a maximum lower cutoff for CBV of 1.5 for radionecrosis and over 1.7 for tumor recurrence with similar radiation-induced lesions to those reported by Barajas et al. [13] (mean rCBV < 1.57 for radionecrosis, > 2.38 for recurrences).

Extravasation of contrast-medium into the extracellular extravascular compartment because of breach of the blood-brain barrier produces an increase in the T1-weighted signal, contrasting with the fall in signal due to the reduction in T2* leading to a fall in the calculated relative CBV [36]. In order to avoid errors due to extravasation of contrast-medium due to the T1-weighted effect, Hu et al. [42] carried out a perfusion study after two injections of gadolinium (6 min and 3 min after a bolus injection) and proposed a cutoff of 0.71 to distinguish recurrence from radionecrosis, with a sensitivity of 91.7% and specificity of 100%. The fall in T1 signal as a result of the earlier injection, however, causes an increase in the T2* susceptibility effect leading to a fall in baseline signal intensity and therefore, a lower estimated percentage signal recovery. An alternative to preliminary injection to counter the contrast-medium extravasation effect on T1 and T2* signals is to optimize the echo time and tilt angle for the perfusion sequence (an echo time of 54 ms to maximize magnetic susceptibility effects and angle of 35° to minimize the T1 effect at 1.5 T), although this carries risks of overestimating the rCBV [43]. New calculation algorithms for hemodynamic response are based on bayesien theory and are now being proposed. These provide a better assessment of blood volume and improve reproducibility [44,45]. Finally, some authors have used other contrast media such as ferumoxytol (iron oxide nanoparticles) which does not extravasate because of the large particle size (up to 50 nm compared to the 1 nm size of the gadolinium chelate) [46].

In the study reported by Barajas et al. [13], the best the first-pass curve parameter to distinguish between lesions

Table 2 Perfusion values from the first-pass technique to distinguish radionecrosis from recurrence of a high-grade glial lesion.

Reference	MF	Population studied			Radionecrosis	Recurrence
		No. of patients	RN	R		
[40]	1.5 T	20	10	10	rCBV < 0.6	rCBV > 2.6
[42]	3 T	13 (40 plvts)	16	24	rCBV < 0.71	rCBV > 0.71
[69]	1.5 T	57	17	40	rpH < 1.38	rpH > 1.38
					rPRS > 87.3%	rPRS < 87.3%
					rCBV mean = 1.57	rCBV mean = 2.38
					rCBV max = 4.63	rCBV max = 8.16
[32]	1.5 T and 3 T	11	6	5	rCBV max < 1.5	rCBV max > 1.7
					rCBV mean < 1	rCBV mean > 1.25

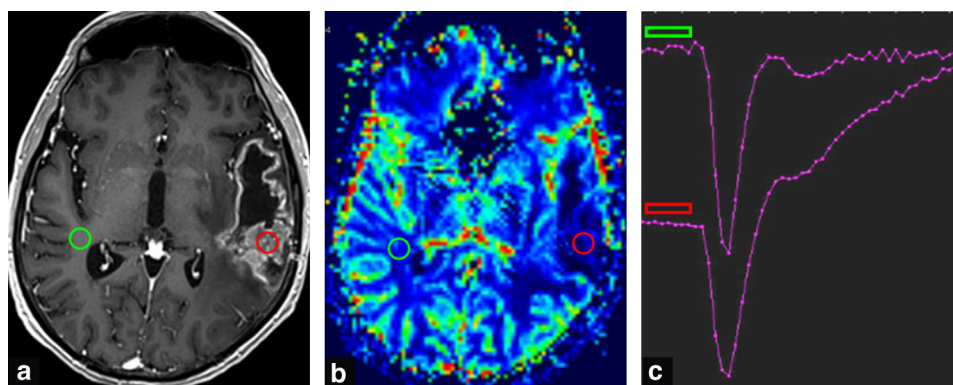MF: magnetic field; RN: radionecrosis; R: recurrence.

Figure 4. Radionecrosis: first-pass gadolinium curve. Left temporal glioblastoma treated with RT and temodal. Repeat MRI performed 3 months after starting RT. Development of a vast area of necrosis of the lesion with new contrast-enhancement. The curve parameters (rCBV = 0.9; PSR = 100; rHP = 0.72) suggest radionecrosis which is confirmed by the secondary regression of the contrast-enhancement.
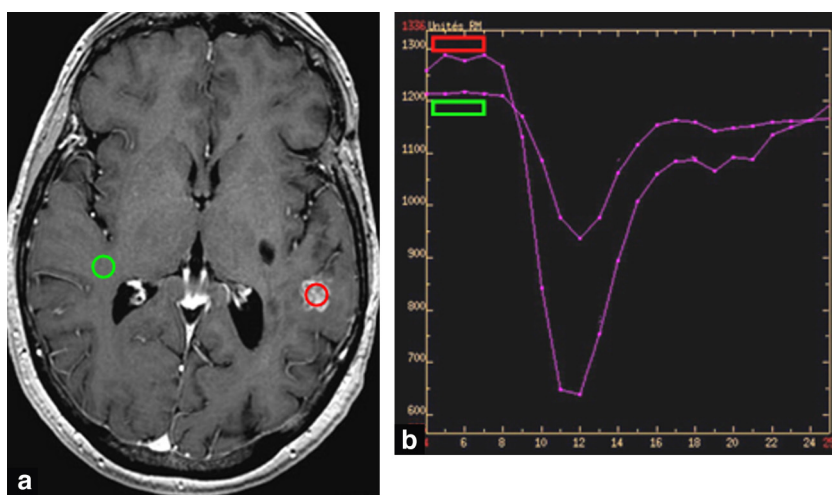
Figure 5. Recurrence of glioblastoma: first-pass gadolinium curve. Appearances of nodular contrast-enhancement above the initial surgical site for the glioblastoma. The curve parameters (rCBV = 0.9; PSR = 0.66; rHP = 2.3) showed tumor neoangiogenesis.

was the relative amplitude of the peak (rPA: relative peak amplitude in the lesion/peak amplitude in the healthy area) (Figs. 4 and 5). This is higher in recurrences, with a cutoff value of 1.38 giving a sensitivity of 89% and specificity of 81%. Another assessment parameter is the relative percentage signal recovery (PSR), which is significantly lower in tumor recurrence: the upper cutoff is 87.3% with a sensitivity of 78% and specificity of 76%.

When contrast uptake occurring in the initial weeks following irradiation occurs and pseudoprogression is being considered, perfusion imaging is also extremely valuable. Mangla et al. [47] found a mean reduction in rCBV of 41% in pseudoprogression compared to a 12% increase in true tumor progression (sensitivity: 77% specificity 86%). In the study by Kong et al. [48], a significant difference was found between mean CBV for pseudoprogression and tumor recurrence: ratio over 1.49 (sensitivity of 81.5% and specificity of 77.8%) for the diagnosis of tumor recurrence and the rCBV was a better index for tumor recurrence if the non-methylated patient.

Finally, the two technical difficulties of perfusion analysis should be remembered:
- EPI echo gradient imaging may be uninterpretable post-operatively because of magnetic susceptibility artifacts due to the metallic material adjacent to the operation site (materials relating to the flap, metal dust left during drilling);
- Differences in perfusion values are seen according to the power of magnetic field and the sequence parameters used: overestimation of the CBV and HP and underestimation of the PT in 3T imaging compared to 1.5T imaging [49].

Study of T1-weighted dynamic enhancement

This technique provides a direct measurement of cerebral blood volumes and flows and the permeability of the blood-brain barrier (using parameters such as the le K_{trans}). It provides absolute blood volume values without the need to correct for the pass contrast curve if the barrier is breached [50] and without the need for a reference region.

In T1-weighed imaging, it is also less sensitive to magnetic susceptibility artifacts. In a pilot study (of 18 patients, 3 patients with radionecrosis), Larsen et al. [51] showed that all lesions which regressed had a CBV of ≤ 1.7 ml/100 g and that all lesions which had progressed or were histologically found to be malignant had a CBV of ≥ 2.2 ml/100 g.

Perfusion analysis by arterial spin labeling (ASL)

In a study comparing ASL findings, first-pass of gadolinium and PET CT, Ozsunar et al. [52] found ASL to offer better diagnostic sensitivity (sensitivities of 88, 86 and 81%) and a proposed 1.3 as the cutoff value for the standardized ASL ratio to distinguish radionecrosis from recurrence. ASL provides an absolute quantification of cerebral blood flow (but not CBV) and is not affected by capillary leakage, which leads to an underestimation of CBV and flow when the curves are analyzed after gadolinium enhancement.

Spectroscopy

Structural tissue degradation after radiotherapy is accompanied by an early change in metabolic activity before the development of neurocognitive symptoms and visible anatomical changes on conventional imaging. Changes in cerebral metabolites particularly involve N acetylaspartate (NAA) which is considered to be a neuronal marker, concentrations of which fall because of cell death by apoptosis or neuronal dysfunction. The second metabolite which is affected by irradiation is choline, levels of which correlate with the biosynthesis of cell membranes and with metabolic turnover. Creatinine (Cr), a marker of energy metabolism, is considered to be relatively stable in radiation damage although this is debated (particularly because of concomitant hypoxic effects) [53]. Classically a small rise in the Cho peak and Cho/Cr ratio is seen in tissue areas involved by radionecrosis (Fig. 6a). Radiation lesions may also display a large peak located between 0.8 and 2.4 ppm which reflects the presence of cell debris containing fatty-acids, lactate and amino-acids [54]. The peaks found between 2.37 and 2.4 ppm in severe post-radiation lesions are due to the
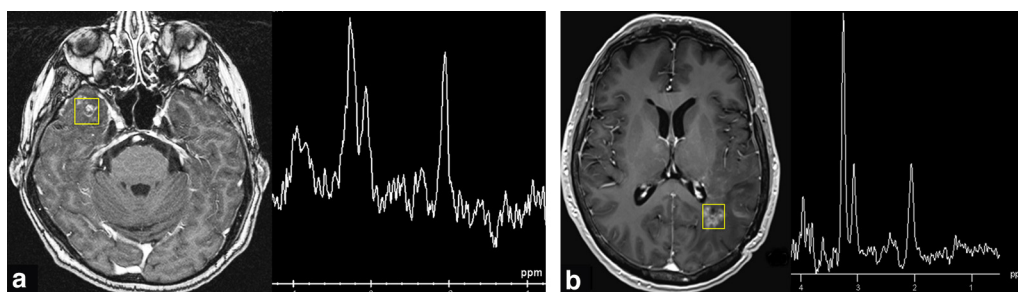
Figure 6. Spectroscopy. a: temporal radionecrosis after whole brain irradiation (monovoxel spectroscopy, TE: 135 ms): Cho/NAA ratio 1.15, inverted lactate peak present. b: tumor recurrence (monovoxel spectroscopy, TE: 135 ms): Cho/NAA ratio 2.3.

presence of co-existent lactate because of anaerobic glycolysis of pyruvate (2.37 ppm) or succinate (2.4 ppm) as is seen in abscesses. Whilst tumor recurrences are also associated with a fall in NAA, they do however display a large rise in the Cho peak because of cellular proliferation (Fig. 6b).

The most widely used ratios in the literature are Cho/Cr and Cho/NAA [55,57] (Table 3). Elias et al. [58]

showed that non-standardized ratios (with the lesion metabolites used as the denominator) correlated far more strongly with the diagnosis than standardized ratios (the metabolite in the ''normal'' contralateral hemisphere used as the denominator). Cutoff values vary depending on the study (from 0.7 to 2 for Cho/Cr). These differences are probably due to small numbers, heterogeneous

Table 3 Spectroscopic studies for the differential diagnosis between radionecrosis and recurrence of a high-grade glial lesion.

	MF	Spectroscopy	Population studies			References	Studies
			No. of patients	RN	R		
Kimura et al., 2001	1.5T	Monovoxel	26	7	19	Cho/Cr < 2.48	Cho/Cr > 2.38
Schlemmer et al., 2001	1.5T	Monovoxel	50 (66 samples)	32	34	ItCho/ItCr = 1.26 ± 0.61 ItCho/INAA = 1.29 ± 1.17	ItCho/ItCr = 2.30 ± 1.2 ItCho/INAA = 3.44 ± 2.76
Rock et al., 2002 [59]	1.5T	Multivoxels	Total = 27 (42 spectros)	15	27	Cho/nCr < 0.89 Cho/nCho < 0.66 Lip-Lac/Cho > 1.36 Lip-Lac/nCr > 2.84 Lip-Lac/Cho < 0.75	Cho/nCr > 1.79
Rock et al., 2004	1.5T	Multivoxels	18 (65 spectros)	33	28	Cho/NAA < 0.2 NAA/nCr > 1.56 NAA/Cho > 1.32	
Webright et al., 2005 [60]	1.5T	Multivoxels	30	12	18	rCho/Cr = 1.52 rCho/NAA = 1.31 rmean NAA/Cr = 1.22	rCho/Cr = 2.52 rCho/NAA = 3.48 rmoy/NAA/
Zeng et al., 2006 [29]	3T	Multivoxels	55	23	32	Cho/Cr = 1.61 Cho/NAA = 1.55 Lac/Cr = 0.45 Lip/Cr = 0.54 NAA/Cr = 1.1	Cho/Cr = 2.82 Cho/NAA = 3.52
Zeng et al., 2007 [57]	3T	Multivoxels	28	9	19		Cho/NAA and Cho/Cr > 1.71
Smith et al., 2009 [56]	1.5T	Multivoxels	33	13	20	Cho/NAA < 1.1	Cho/NAA > 2.3

tumors and the difference in techniques used (mono or multivoxel).

Spectroscopic analysis has several limitations:lesions close to bone [13] are difficult to study reliably because of magnetic susceptibility artifacts.

Whilst spectroscopy is reliable to distinguish tissues containing pure radionecrosis or a pure recurrence, it is often difficult to interpret because of the frequent co-existence of radiation lesions and tumor recurrence [59]. The metabolite values are therefore averaged within the voxel taking account of false negatives for tumor recurrence. In addition, monovoxel studies only provide a partial metabolic investigation enhancing large or multifocal areas. Multivoxel spectroscopy can therefore show tumor profiles in areas which do not enhance and in the apparently neighboring white matter [60].

After treatment of a cerebral metastasis

Conventional imaging

A transient increase in volume of over 20% of the pre-treatment volume is seen in a third of cases after stereotactic RT for cerebral metastases [61]. This increase in size may begin from 6 weeks after radiotherapy and last for up to 15 months [61]. It is more common in men and if the irradiated volume is over 5 cm^3 [62]. The natural history of these changes in volume varies depending on whether or not the primary tumor is radiosensitive: metastases from radiosensitive tumors (lung, breasts and colon) display a transient increase in volume (peaking between 12 and 18 months after radiotherapy) whereas the volumes of metastases from non-radiosensitive tumors remain relatively stable. The great majority of these increases in volume is asymptomatic and only requires monitoring.

In the study by Patel et al. [61], this transient increase in size carried a good prognosis: when present, patients had longer median survival (> 18.4 months) than those whose lesions remained stable or reduced in size (16.4 months). This may be due to the immune reaction associated with the inflammation and necrosis seen in these radiation reactions, as strong immune responses are associated with increased survival and control of cancers [63].

In general, the transient increase in volume post-radiation is modest: an increase of more than 65% compared to the volume of the first post-treatment review suggests a recurrence or continued tumor activity (sensitivity: 100%, specificity 80%) [64] (Fig. 7).

Several studies have compared the appearances of enhanced T2-weighted and T1-weighted lesions. Dequesada et al. [7] compared the area of the visible nodule on T2-weighted spin echo images (AT2) to the area visible on the T1-weighted image after gadolinium (AT1Gd). An AT2/AT1Gd radio of 0.3 or less suggested radionecrosis (4 of the 5 cases of radionecrosis) whereas all of the pure tumor recurrences (7 cases) had a ratio of over 0.6. The post-irradiation inflammatory infiltrate displays an obvious hyperintensity on T2-weighted imaging, unlike the T2-weighted hypointensity which a number of metastases display. It should be noted, however, that most of the investigations are currently performed using T2 flair sequences in which most metastases appear as hyperintense, therefore limiting the value of this ratio. In addition, these results were not confirmed in the more recent study conducted by Stockham et al. [65] (51 patients with histological confirmation, including 13 cases of radionecrosis) in which the lesion quotient only provided a sensitivity of 8% (specificity 91%).

Another more qualitative method is based on the correlation between the boundaries of the lesion seen on enhanced T1-weighted and T2-weighted imaging [66]. Correlations reflect tumor recurrence and non-correlations ("T1/T2 mismatch") reflect radionecrosis (Fig. 8, Fig. 9). The sensitivity of the "T1/T2 mismatch" in this study was 83% with a specificity of 91%.

The amount of edema present on T2-weighted imaging has also been studied with calculation of the T2-weighted hyperintensity volume/T1 weighed volume after enhancement. When over 10, this had a positive predictive value of 92% for radionecrosis [67].
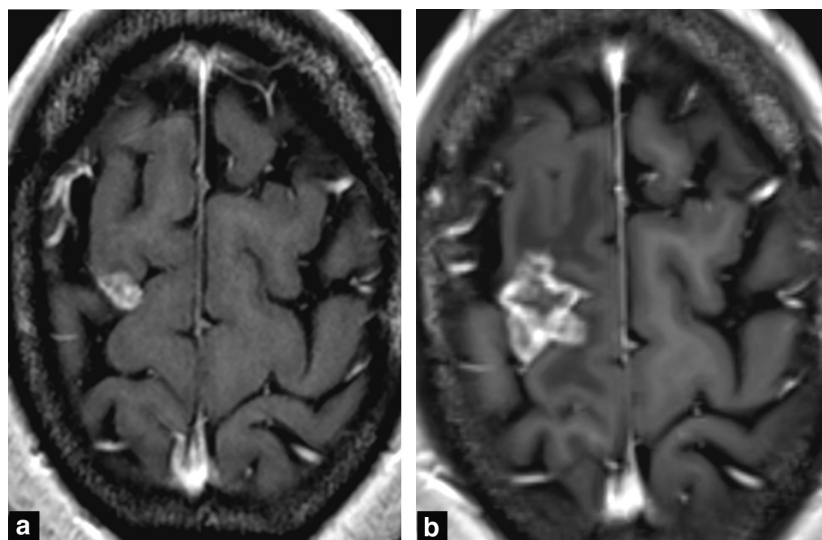

Figure 7. Active progression of a metastasis. T1-weighted axial images after gadolinium 12 (a) and 15 months (b) after radiotherapy for a right frontal metastasis. Large increase in volume of the lesion (> 65%) representing active recurrence.
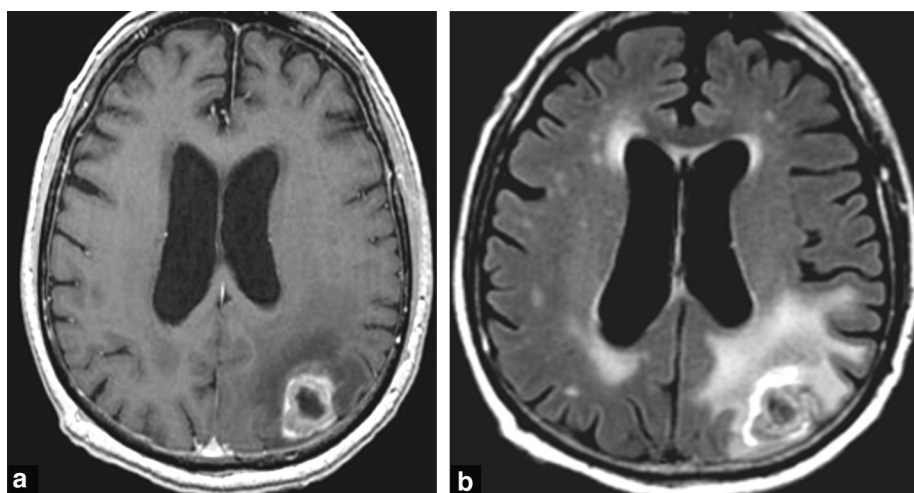
Figure 8. Analysis of the T2/T1Gd ratio: active progression of a metastasis. T1-weighted axial (a) and T2 flair (b) images after gadolinium. Good correlation between lesion boundaries seen on T1 with enhancement and in T2 (no T1/T2 mismatch). Significant perilesional edema on the T2-weighted series.

The morphological appearances of contrast uptake (irregular, annular or nodular) are non-specific. This includes the ''sliced leak'' appearance described by Dequesada et al. [7] as being suggestive of a diagnosis of radionecrosis, although this has not been found by other authors [64].

Perfusion imaging

On electron microscopy, the ultrastructure of the tumor capillaries of cerebral metastases resembles more that of the original tumor than the cerebral tissue capillaries. These tumor vessels display increased tortuosity, lack of maturity and increased permeability. In addition, as they do not have the blood-brain barrier of the native cerebral capillaries, they are very permeable to macromolecular contrast agents.

Analysis of perfusion images in the literature has been based on relative cerebral blood volume (rCBV), the relative amplitude of the peak (rHP) and the percentage signal recovery (PSR) [64,68,69]. All authors have found a significant increase in average and maximum rCBV in the group

of patients with metastatic recurrence (the best cutoff values range from 1.52 to 2.1 depending on the studies [64,68] (Fig. 10, Fig. 11). rCBV values of < 1.35 were only seen in the group of patients with irradiation lesions in the study reported by Barajas et al. [69].

The large overlap of CBV values may be explained by:
- tumor heterogeneity;
- inability to distinguish the rise in microvascular density from metastatic recurrences from post-radiation changes in vascularization which involve hyper-plastic dilated blood vessels;
- the co-existence of radionecrosis lesions with tumor recurrence (50% radionecrotic tissue in tissue samples from metastatic recurrence);
- magnetic susceptibility artifacts due to petechial hemorrhage caused by the irradiation, which artificially reduce the rCBV of a recurrence. Similarly, in metastases of melanoma, melanin may as an artifact impede the analysis of the CBV.
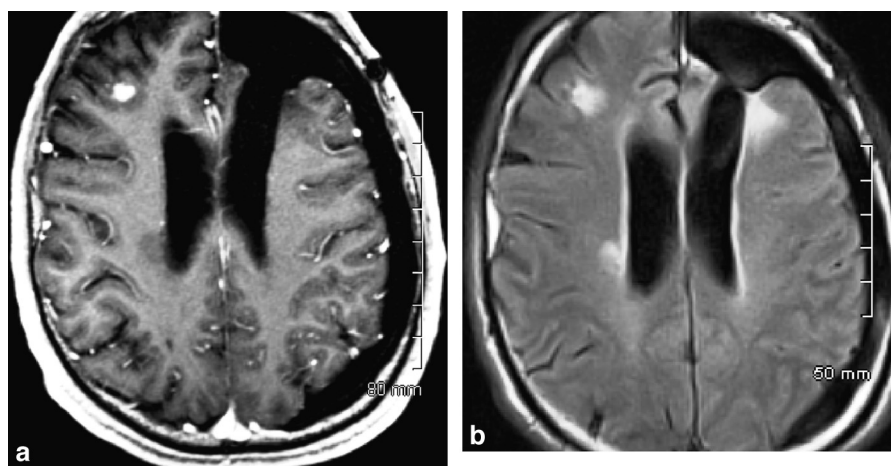

Figure 9. Analysis of the T2/T1Gd ratio: radionecrosis. T1 (a) and T2 flair (b) axial images after gadolinium. Poor correlation between lesion boundaries seen on T1 with enhancement and in T2-weighted images (T1/T2 mismatch). Relatively insignificant perilesional edema on the T2-weighted series.
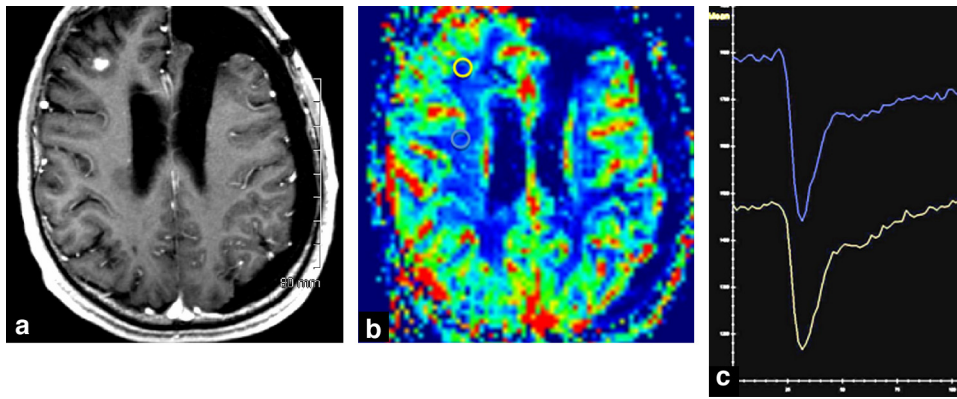
Figure 10. Perfusion study using the first-pass technique: radionecrosis. T1-weighted axial image after gadolinium (a), cerebral blood volume mapping (b), first-pass curves (c). Parameters obtained from the curve for the PSR lesion = 77%, rCBV = 1, rPH = 0.8.

The ratio of peak amplitudes is also higher in tumor recurrence, although these values are no more discriminatory than the CBV.

According to Barajas et al. [69] studying the PSR better separated metastatic recurrence from radionecrosis lesions. These authors proposed a PSR cutoff value of 76.3% supporting radionecrosis lesions, with a sensitivity of 95.65% and a specificity of 100%. Lower PSR values which indicate microvascular leakage in metastatic recurrences probably reflect the increase in capillary permeability of tumor vessels.

Spectroscopy

Huang et al. [64] assessed spectroscopy to distinguish metastatic recurrence from radionecrosis. A choline ratio (rCho = Cho lesion/Cho contralateral healthy area) of over 1.2 suggested a tumor recurrence (with a sensitivity of 33% and specificity of 100%) and was of better diagnostic value than the conventional ratios (Cho/Cr and Cho/NAA).

Chernov et al. [70] primarily used the lipid/Cho ratio and found that a value of 3 or a large fall in all of the peaks suggested radionecrosis, whereas a lipid/Cho ratio of under 3 combined with a NAA/Cho ratio of under 1 was seen in tumor recurrence (sensitivity of 50% and specificity 100% in this study).

The main criteria for differential diagnosis by MR are summarized in Table 4.

Scintigraphy investigations

18F-fluorodeoxyglucose has been studied in PET CT, based on the premise that the uptake of tracer is increased by tumor metabolism and reduced in radionecrosis. In this case the diagnostic sensitivity of scintigraphy has been reported to be 75%, with a specificity of 80% [71]. Interpretation of 18F-FDG-PET CT is hindered by the large physiological cortical metabolic activity and false positive results may occur with abscesses and from the inflammation caused by radionecrosis.

Other tracers can be used in PET CT in this situation, including amino-acids (methionine, tyrosine and choline) and nucleosides (fluorothymidine). These tracers are involved in protein synthesis and are good indicators of cells in the proliferative phase. The extent of their uptake correlates with disease activity or tumor regrowth. They are complicated to use when bound to C11 as this has a half-life of 20 min limiting its use to centers located close to a cyclotron, radiochemistry laboratories and the radiopharmacy required for their production. These tracers have been tested and shown sensitivity of 95—100% and a specificity of 80 to 100% [72].
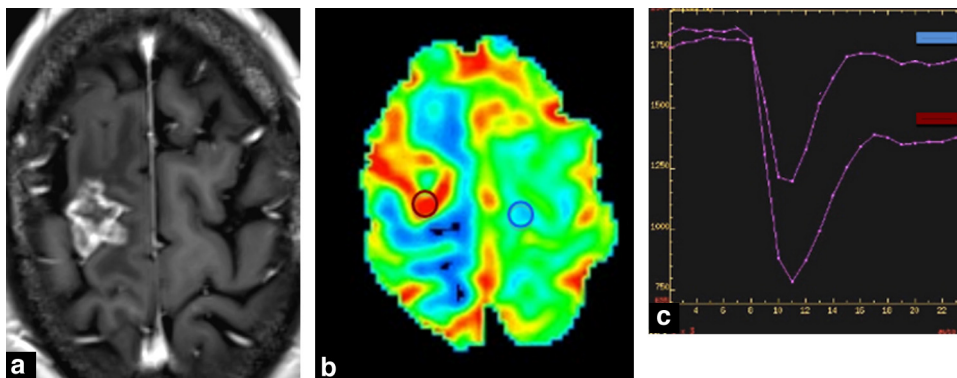

Figure 11. Perfusion study using the first-pass technique: active progression of a metastasis. T1-weighted axial image after gadolinium (a), cerebral blood volume mapping (b), first-pass curves (c), parameters obtained from the curve for the PSR lesion = 53%, rCBV = 2.6; rPH = 1.75.

Table 4 Main MRI criteria for the differential diagnosis between radionecrosis and metastases.

MRI	Radionecrosis	Recurrence	Reference
Conventional sequences	Nodule area T2/T1 gado+ $\leq$ 0.3 T1—T2: tissue boundaries comparable edema volume/lesion > 10	Nodule area T2/T1 gado+ $\leq$ 0.6 T1—T2 mismatch Volume edema/lesion < 10 Increased volume > 65%	Dequesada et al., 2008 Stockham et al., 2012 Kano et al., 2010 Leeman et al., 2013 Huang et al., 2008 Barajas et al., 2009
Perfusion imaging	rCBV < 1.54	PSR < 76.3%	
Spectroscopy	Lipids/Cho > 3 or very low peaks	rCBV > 2 rCBV > 2.1 lipids/Cho < 3 and NAA/Cho < 1 rCho > 1.2	Huang et al., 2008 Mitsuya et al., 2010 Chernov et al., 2006 Huang et al., 2008

The tracers can now be labeled with fluorine 18, as in 18F-fluoroethyltyrosine, which greatly facilitates their use and the wider use of this technique [73].

Other nuclear medicine methods such as thallium-201 SPECT are also used and offer a sensitivity and specificity of 90% [74]. These scintigraphic methods are particularly useful when magnetic susceptibility artifacts are present on MR, preventing interpretation of advanced MR techniques [75].

Treatment of radionecrosis

At present, there is no specific medical treatment for radionecrosis. Corticosteroids are usually started in order to reduce the edema and inflammatory components associated with the radionecrosis, and hyperbaric oxygen therapy has been proposed as both a curative and preventative treatment [76]. Bevacizumab (Avastin®) in particularhas been shown to be effective in reducing radionecrosis lesions because of its anti-angiogenic (anti-VEGF) properties [77—79]. It also has an antineoplastic effect which may be of use if radiological progression remains uncertain [80].

Radionecrosis lesions occasionally need to be excised surgically because of a symptomatic space-occupying lesion effect or if diagnostic doubt is present about lesions located in a non-functional area [81].

Conclusion

Developing or increasing MRI contrast-enhancement in an irradiated tumor site raises the question of the differential diagnosis between tumor recurrence and radionecrosis. In view of the therapeutic and prognostic challenges, it is important that the MRI conclusion can point towards one of these diagnoses from the beginning. With irradiated glial lesions the morphology of contrast-enhancement cannot guide the diagnosis and perfusion and spectroscopy techniques (if possible using multivoxels) are required. During the follow-up of metastases, a transient moderate increase in lesion volume may occur and carry a good prognosis. The morphological features (volume, T2/T1Gd ratio) and perfusion features can guide towards the diagnosis. The different factors pointing towards the most appropriate diagnosis of radionecrosis on MRI criteria are summarized in Fig. 12. A diagnostic, clinical and radiological approach is proposed when the differential diagnosis between radionecrosis and recurrence remains problematic (Fig. 13).
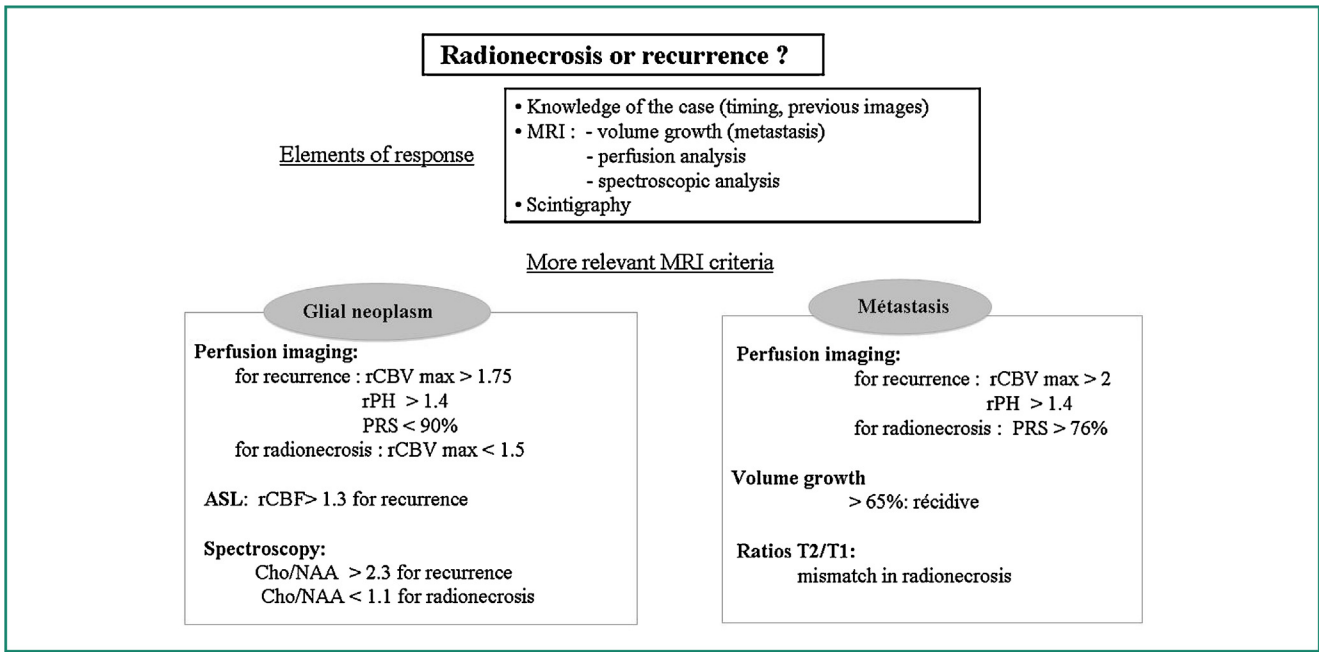
Radionecrosis or recurrence ?

Elements of response

- Knowledge of the case (timing, previous images)
- MRI : - volume growth (metastasis)
  - perfusion analysis
  - spectroscopic analysis
- Scintigraphy

More relevant MRI criteria

Glial neoplasm

Perfusion imaging:
for recurrence : rCBV max > 1.75
rPH > 1.4
PRS < 90%
for radionecrosis : rCBV max < 1.5

ASL: rCBF> 1.3 for recurrence

Spectroscopy:
Cho/NAA > 2.3 for recurrence
Cho/NAA < 1.1 for radionecrosis

Métastasis

Perfusion imaging:
for recurrence : rCBV max > 2
rPH > 1.4
for radionecrosis : PRS > 76%

Volume growth
> 65%: récidive

Ratios T2/T1:
mismatch in radionecrosis

Figure 12. Elements of response for radionecrosis. More relevant MRI criteria.

Recurrence or Radionecrosis ?

MRI
- Volumetry
- Perfusion
- Spectroscopy

Possible radionecrosis → Recurrence

Scintigraphy

- Discussion of corticosteroids
- Close clinical and radiological follow-up
  - Radiological reassessment (4-6 weeks) on the same scanner
  - Multimodal MRI (T1Gd, Flair, T2*, perfusion and spectroscopy)

Radionecrosis | Doubtful | Recurrence

Continuation of monitoring (MRI /3 month) | Biopsy or exérèse
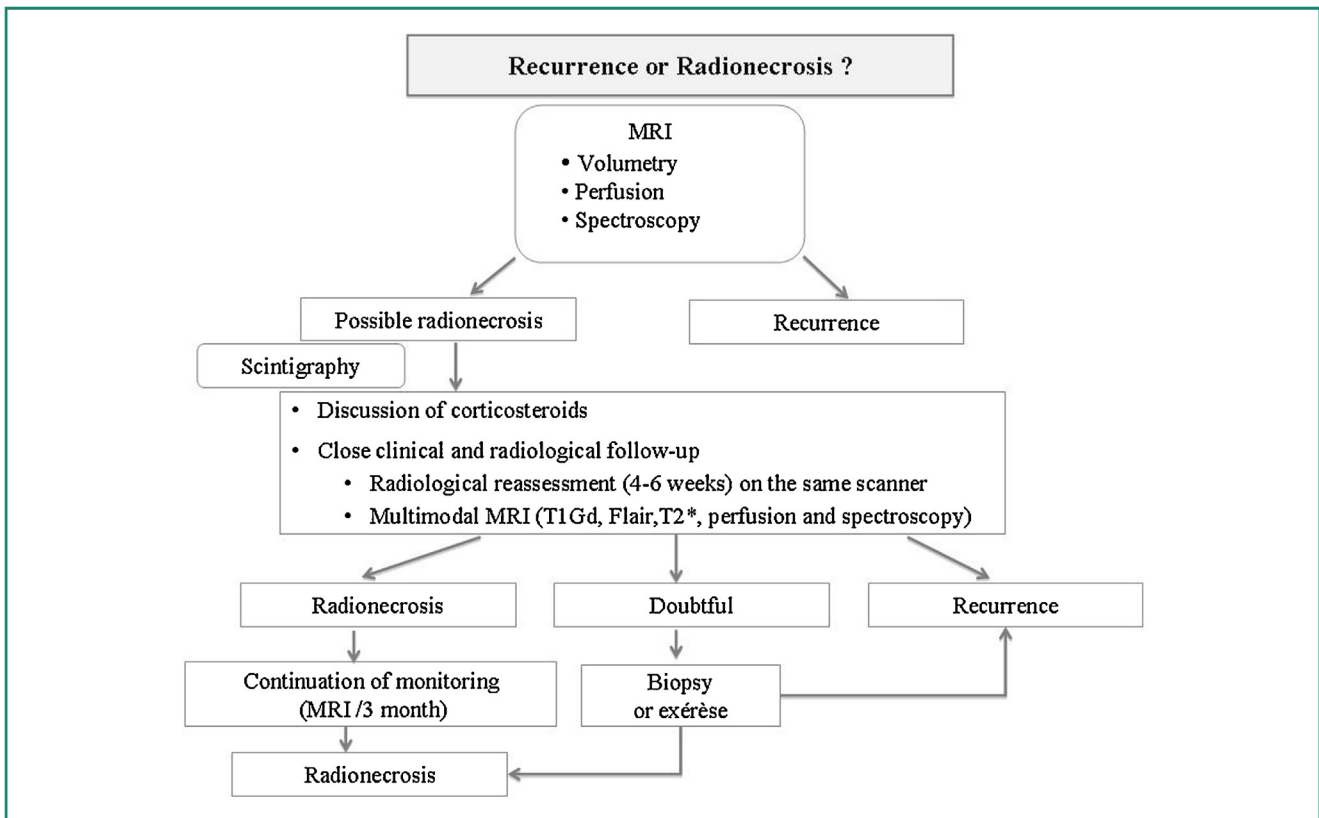
Radionecrosis

Figure 13. Clinical and radiological approach for the differential diagnosis between radionecrosis and tumor recurrence.

TAKE-HOME MESSAGES

- There is currently no morphological criterion to separate with certainty radionecrosis and recurrent glioblastoma.
- In the follow-up of radiosurgery for brain metastasis, a transient and moderate increase of the lesion volume is possible with a good prognosis, but an important volume increase is a sign of recurrence.
- Corresponding limits of the lesion on T2 and T1 gadolinium sequences was in favor of a metastatic recurrence.
- It is essential to add advanced techniques sequences (perfusion, spectroscopy, diffusion) in the MR protocol in an attempt to differentiate radiation injury from tumor recurrence.
- These advanced techniques can be difficult to interpret given the heterogeneity of radionecrosis lesions and the frequent association of these lesions with evolving tumor tissues.
- The perfusion imaging (CBV and percent recovery of the signal) is currently the most reliable MR method to separate radionecrosis from tumor recurrence.

Disclosure of interest

The authors declare that they have no conflicts of interest concerning this article.

References

[1] Tabouret E, Bauchet L, Carpentier A. Brain metastases epidemiology and biology. Bull Cancer 2013;100(1):57—62.

[2] Omuro A, DeAngelis LM. Glioblastoma and other malignant gliomas: a clinical review. JAMA 2013;310(17):1842—50.

[3] Kumar AJ, Leeds NE, Fuller GN, Van Tassel P, Maor MH, Sawaya RE, et al. Malignant gliomas: MR imaging spectrum of radiation therapy- and chemotherapy-induced necrosis of the brain after treatment. Radiology 2000;217(2):377—84.

[4] Ruben JD, Dally M, Bailey M, Smith R, McLean CA, Fedele P. Cerebral radiation necrosis: incidence, outcomes, and risk factors with emphasis on radiation parameters and chemotherapy. Int J Radiat Oncol Biol Phys 2006;65(2):499—508.

[5] Minniti G, Clarke E, Lanzetta G, Osti MF, Trasimeni G, Bozzao A, et al. Stereotactic radiosurgery for brain metastases: analysis of outcome and risk of brain radionecrosis. Radiat Oncol 6:48.

[6] Kimura T, Sako K, Tanaka K, Gotoh T, Yoshida H, Aburano T, et al. Evaluation of the response of metastatic brain tumors to stereotactic radiosurgery by proton magnetic resonance spectroscopy, 201TlCl single-photon emission computerized tomography, and gadolinium-enhanced magnetic resonance imaging. J Neurosurg 2004;100(5):835—41.

[7] Dequesada IM, Quisling RG, Yachnis A, Friedman WA. Can standard magnetic resonance imaging reliably distinguish recurrent tumor from radiation necrosis after radiosurgery for brain metastases? A radiographic-pathological study. Neurosurgery 2008;63(5):898—904.

[8] Asao C, Korogi Y, Kitajima M, Hirai T, Baba Y, Makino K, et al. Diffusion-weighted imaging of radiation-induced brain injury for differentiation from tumor recurrence. Am J Neuroradiol 2005;26(6):1455—60.

[9] Yoshii Y, Sugimoto K, Fujiwara K. Progressive enlargement of a mass lesion in late cerebral radionecrosis. J Clin Neurosci 2011;18(6):853—5.

[10] Nonoguchi N, Miyatake S-I, Fukumoto M, Furuse M, Hiramatsu R, Kawabata S, et al. The distribution of vascular endothelial growth factor-producing cells in clinical radiation necrosis of the brain: pathological consideration of their potential roles. J Neurooncol 2011;105(2):423—31.

[11] Castel JC, Caillé JM. Imaging of irradiated brain tumours. Value of magnetic resonance imaging. J Neuroradiol 1989;16(2):81—132.

[12] Di Chiro G, Oldfield E, Wright DC, De Michele D, Katz DA, Patronas NJ, et al. Cerebral necrosis after radiotherapy and/or intraarterial chemotherapy for brain tumors: PET and neuropathologic studies. AJR Am J Roentgenol 1988;150(1):189—97.

[13] Barajas RF, Chang JS, Segal MR, Parsa AT, McDermott MW, Berger MS, et al. Differentiation of recurrent glioblastoma multiforme from radiation necrosis after external beam radiation therapy with dynamic susceptibility-weighted contrast-enhanced perfusion MR imaging1. Radiology 2009;253(2):486—96.

[14] Forsyth PA, Kelly PJ, Cascino TL, Scheithauer BW, Shaw EG, Dinapoli RP, et al. Radiation necrosis or glioma recurrence: is computer-assisted stereotactic biopsy useful? J Neurosurg 1995;82(3):436—44.

[15] Lee AWM, Kwong DLW, Leung SF, Tung SY, Sze WM, Sham JST, et al. Factors affecting risk of symptomatic temporal lobe necrosis: significance of fractional dose and treatment time. Int J Radiat Oncol Biol Phys 2002;53(1):75—85.

[16] Shaw E, Scott C, Souhami L, Dinapoli R, Kline R, Loeffler J, et al. Single dose radiosurgical treatment of recurrent previously irradiated primary brain tumors and brain metastases: final report of RTOG protocol 90-05. Int J Radial Oncol Biol Phys 2000;47(2):291—8.

[17] Blonigen BJ, Steinmetz RD, Levin L, Lamba MA, Warnick RE, Breneman JC. Irradiated volume as a predictor of brain radionecrosis after linear accelerator stereotactic radiosurgery. Int J Radiat Oncol Biol Phys 2010;77(4):996—1001.

[18] Korytko T, Radivoyevitch T, Colussi V, Wessels B, Pillai K, Maciunas R, et al. 12 Gy gamma knife radiosurgical volume is a predictor for radiation necrosis in non-AVM intracranial tumors. Int J Radiat Oncol Biol Phys 2006;64(2):419—24.

[19] Peca C, Pacelli R, Elefante A, Del Basso De Caro ML, Vergara P, Mariniello G, et al. Early clinical and neuroradiological worsening after radiotherapy and concomitant temozolomide in patients with glioblastoma: tumour progression or radionecrosis? Clin Neurol Neurosurg 2009;111(4):331—4.

[20] Marks JE, Wong J. The risk of cerebral radionecrosis in relation to dose, time and fractionation. A follow-up study. Prog Exp Tumor Res 1985;29:210—8.

[21] Stupp R, Mason WP, van den Bent MJ, Weller M, Fisher B, Taphoorn MJB, et al. Radiotherapy plus concomitant and adjuvant temozolomide for glioblastoma. N Engl J Med 2005;352(10):987—96.

[22] Brandsma D, Stalpers L, Taal W, Sminia P, van den Bent MJ. Clinical features, mechanisms, and management of pseudoprogression in malignant gliomas. Lancet Oncol 2008;9(5):453—61.

[23] Brandes AA, Franceschi E, Tosoni A, Blatt V, Pession A, Tallini G, et al. MGMT promoter methylation status can predict the incidence and outcome of pseudoprogression after concomitant radiochemotherapy in newly diagnosed glioblastoma patients. J Clin Oncol 2008;26(13):2192—7.

[24] Hygino da Cruz Jr LC, Rodriguez I, Domingues RC, Gasparetto EL, Sorensen AG. Pseudoprogression and pseudoresponse: imaging challenges in the assessment of post-treatment glioma. AJNR Am J Neuroradiol 2011;32(11):1978—85.

[25] Moody DM, Bell MA, Challa VR. Features of the cerebral vascular pattern that predict vulnerability to perfusion or oxygenation deficiency: an anatomic study. AJNR Am J Neuroradiol 1990;11(3):431—9.

[26] Mullins ME, Barest GD, Schaefer PW, Hochberg FH, Gonzalez RG, Lev MH. Radiation necrosis versus glioma recurrence: conventional MR imaging clues to diagnosis. AJNR Am J Neuroradiol 2005;26(8):1967—72.

[27] Reddy K, Westerly D, Chen C. MRI patterns of T1 enhancing radiation necrosis versus tumour recurrence in high-grade gliomas. J Med Imaging Radiat Oncol 2013;57(3):349—55.

[28] Chan Y, Leung S, King AD, Choi PHK, Metreweli C. Late radiation injury to the temporal lobes: morphologic evaluation at MR imaging1. Radiology 1999;213(3):800—7.

[29] Zeng Q-S, Kang X-S, Li C-F, Zhou G-Y. Detection of hemorrhagic hypointense foci in radiation injury region using susceptibility-weighted imaging. Acta Radiol 2011;52(1):115—9.

[30] Hein PA, Eskey CJ, Dunn JF, Hug EB. Diffusion-weighted imaging in the follow-up of treated high-grade gliomas: tumor recurrence versus radiation injury. AJNR Am J Neuroradiol 2004;25(2):201—9.

[31] Sundgren PC. MR spectroscopy in radiation injury. Am J Neuroradiol 2009;30(8):1469—76.

[32] Bobek-Billewicz B, Stasik-Pres G, Majchrzak H, Zarudzki L. Differentiation between brain tumor recurrence and radiation injury using perfusion, diffusion-weighted imaging and MR spectroscopy. Folia Neuropathol 2010;48(2):81—92.

[33] Chan Y, Yeung DKW, Leung S, Chan P. Diffusion-weighted magnetic resonance imaging in radiation-induced cerebral necrosis. Apparent diffusion coefficient in lesion components. J Comput Assist Tomogr 2003;27(5):674—80.

[34] Castillo M, Smith JK, Kwock L, Wilber K. Apparent diffusion coefficients in the evaluation of high-grade cerebral gliomas. AJNR Am J Neuroradiol 2001;22(1):60—4.

[35] Sinha S, Bastin ME, Whittle IR, Wardlaw JM. Diffusion tensor MR imaging of high-grade cerebral gliomas. AJNR Am J Neuroradiol 2002;23(4):520—7.

[36] Kitahara S, Nakasu S, Murata K, Sho K, Ito R. Evaluation of treatment-induced cerebral white matter injury by using diffusion tensor MR imaging: initial experience. AJNR Am J Neuroradiol 2005;26(9):2200—6.

[37] Kashimura H, Inoue T, Beppu T, Ogasawara K, Ogawa A. Diffusion tensor imaging for differentiation of recurrent brain tumor and radiation necrosis after radiotherapy — three case reports. Clin Neurol Neurosurg 2007;109(1):106—10.

[38] Sundgren PC, Fan X, Weybright P, Welsh RC, Carlos RC, Petrou M, et al. Differentiation of recurrent brain tumor versus radiation injury using diffusion tensor imaging in patients with new contrast-enhancing lesions. Magn Reson Imaging 2006;24(9):1131—42.

[39] Lupo JM, Cha S, Chang SM, Nelson SJ. Dynamic susceptibility-weighted perfusion imaging of high-grade gliomas: characterization of spatial heterogeneity. AJNR Am J Neuroradiol 2005;26(6):1446—54.

[40] Sugahara T, Korogi Y, Tomiguchi S, Shigematsu Y, Ikushima I, Kira T, et al. Posttherapeutic intra-axial brain tumor: the value of perfusion-sensitive contrast-enhanced MR imaging for differentiating tumor recurrence from nonneoplastic contrast-enhancing tissue. AJNR Am J Neuroradiol 2000;21(5):901—9.

[41] Spiegelmann R, Friedman WA, Bova FJ, Theele DP, Mickle JP. LINAC radiosurgery: an animal model. J Neurosurg 1993;78(4):638—44.

[42] Hu LS, Baxter LC, Smith KA, Feuerstein BG, Karis JP, Eschbacher JM, et al. Relative cerebral blood volume values to differentiate high-grade glioma recurrence from post-treatment radiation effect: direct correlation between image-guided tissue histopathology and localized dynamic

susceptibility-weighted contrast-enhanced perfusion MR imaging measurements. AJNR Am J Neuroradiol 2009;30(3):552—8.

[43] Paulson ES, Schmainda KM. Comparison of dynamic susceptibility-weighted contrast-enhanced MR methods: recommendations for measuring relative cerebral blood volume in brain tumors. Radiology 2008;249(2):601—13.

[44] Kudo K, Christensen S, Sasaki M, Østergaard L, Shirato H, Ogasawara K, et al. Accuracy and reliability assessment of CT and MR perfusion analysis software using a digital phantom. Radiology 2013;267(1):201—11.

[45] Boutelier T, Kudo K, Pautot F, Sasaki M. Bayesian hemodynamic parameter estimation by bolus tracking perfusion-weighted imaging. IEEE Trans Med Imaging 2012;31(7):1381—95.

[46] Gahramanov S, Muldoon LL, Varallyay CG, Li X, Kraemer DF, Fu R, et al. Pseudoprogression of glioblastoma after chemo- and radiation therapy: diagnosis by using dynamic susceptibility-weighted contrast-enhanced perfusion MR imaging with ferumoxytol versus gadoteridol and correlation with survival. Radiology 2013;266(3):842—52.

[47] Mangla R, Singh G, Ziegelitz D, Milano MT, Korones DN, Zhong J, et al. Changes in relative cerebral blood volume 1 month after radiation-temozolomide therapy can help predict overall survival in patients with glioblastoma. Radiology 2010;256(2):575—84.

[48] Kong D-S, Kim ST, Kim E-H, Lim DH, Kim WS, Suh Y-L, et al. Diagnostic dilemma of pseudoprogression in the treatment of newly diagnosed glioblastomas: the role of assessing relative cerebral blood flow volume and oxygen-6-methylguanine-DNA-methyltransferase promoter methylation status. AJNR Am J Neuroradiol 2011;32(2):382—7.

[49] Mauz N, Krainik A, Tropres I, Lamalle L, Sellier E, Eker O, et al. Perfusion magnetic resonance imaging: comparison of semio-logic characteristics in first-pass perfusion of brain tumors at 1.5 and 3 Tesla. J Neuroradiol 2012;39(5):308—16.

[50] Larsson HBW, Hansen AE, Berg HK, Rostrup E, Haraldseth O. Dynamic contrast-enhanced quantitative perfusion measurement of the brain using T1-weighted MRI at 3T. J Magn Reson Imaging 2008;27(4):754—62.

[51] Larsen VA, Simonsen HJ, Law I, Larsson HBW, Hansen AE. Evaluation of dynamic contrast-enhanced T1-weighted perfusion MRI in the differentiation of tumor recurrence from radiation necrosis. Neuroradiology 2013;55(3):361—9.

[52] Ozsunar Y, Mullins ME, Kwong K, Hochberg FH, Ament C, Schaefer PW, et al. Glioma recurrence versus radiation necrosis? A pilot comparison of arterial spin-labeled, dynamic susceptibility contrast-enhanced MRI, and FDG-PET imaging. Acad Radiol 2010;17(3):282—90.

[53] Walecki J, Sokól M, Pieniazek P, Maciejewski B, Tarnawski R, Krupska T, et al. Role of short TE 1H-MR spectroscopy in monitoring of postoperation irradiated patients. Eur J Radiol 1999;30(2):154—61.

[54] Yeung DK, Chan Y, Leung S, Poon PM, Pang C. Detection of an intense resonance at 2.4 ppm in 1H-MR spectra of patients with severe late-delayed, radiation-induced brain injuries. Magn Reson Med 2001;45(6):994—1000.

[55] Amin A, Moustafa H, Ahmed E, El-Toukhy M. Glioma residual or recurrence versus radiation necrosis: accuracy of pentavalent technetium-99m-dimercaptosuccinic acid [Tc-99m (V) DMSA] brain SPECT compared to proton magnetic resonance spectroscopy ((1)H-MRS): initial results. J Neurooncol 2012;106(3):579—87.

[56] Smith EA, Carlos RC, Junck LR, Tsien CI, Elias A, Sundgren PC. Developing a clinical decision model: MR spectroscopy to differentiate between recurrent tumor and radiation change in patients with new contrast-enhancing lesions. AJR Am J Roentgenol 2009;192(2):W45—52.

[57] Zeng Q-S, Li C-F, Liu H, Zhen J-H, Feng D-C. Distinction between recurrent glioma and radiation injury using magnetic resonance

spectroscopy in combination with diffusion-weighted imaging. Int J Radiat Oncol Biol Phys 2007;68(1):151—8.

[58] Elias AE, Carlos RC, Smith EA, Frechtling D, George B, Maly P, et al. MR spectroscopy using normalized and non-normalized metabolite ratios for differentiating recurrent brain tumor from radiation injury. Acad Radiol 2011;18(9):1101—8.

[59] Rock JP, Hearshen D, Scarpace L, Croteau D, Gutierrez J, Fisher JL, et al. Correlations between magnetic resonance spectroscopy and image-guided histopathology, with special attention to radiation necrosis. Neurosurgery 2002;51(4):912—9.

[60] Weybright P, Sundgren PC, Maly P, Hassan DG, Nan B, Rohrer S, et al. Differentiation between brain tumor recurrence and radiation injury using MR spectroscopy. AJR Am J Roentgenol 2005;185(6):1471—6.

[61] Patel TR, McHugh BJ, Bi WL, Minja FJ, Knisely JPS, Chiang VL. A comprehensive review of MR imaging changes following radiosurgery to 500 brain metastases. AJNR Am J Neuroradiol 2011;32(10):1885—92.

[62] Peterson AM, Meltzer CC, Evanson EJ, Flickinger JC, Kondziolka D. MR imaging response of brain metastases after gamma knife stereotactic radiosurgery. Radiology 1999;211(3):807—14.

[63] Hamaï A, Benlalam H, Meslin F, Hasmim M, Carré T, Akalay I, et al. Immune surveillance of human cancer: if the cytotoxic T-lymphocytes play the music, does the tumoral system call the tune? Tissue Antigens 2010;75(1):1—8.

[64] Huang J, Wang AM, Shetty A, Maitz AH, Yan D, Doyle D, et al. Differentiation between intra-axial metastatic tumor progression and radiationinjury following fractionated radiation therapy or stereotactic radiosurgery using MR spectroscopy, perfusion MR imaging or volume progression modeling. Magn Reson Imaging 2011;29(7):993—1001.

[65] Stockham AL, Tievsky AL, Koyfman SA, Reddy CA, Suh JH, Vogelbaum MA, et al. Conventional MRI does not reliably distinguish radiation necrosis from tumor recurrence after stereotactic radiosurgery. J Neurooncol 2012;109(1):149—58.

[66] Kano H, Kondziolka D, Lobato-Polo J, Zorro O, Flickinger JC, Lunsford LD. T1/T2 matching to differentiate tumor growth from radiation effects after stereotactic radiosurgery. Neurosurgery 2010;66(3):486—91.

[67] Leeman JE, Clump DA, Flickinger JC, Mintz AH, Burton SA, Heron DE. Extent of perilesional edema differentiates radionecrosis from tumor recurrence following stereotactic radiosurgery for brain metastases. Neuro Oncol 2013;15(12):1732—8.

[68] Mitsuya K, Nakasu Y, Horiguchi S, Harada H, Nishimura T, Bando E, et al. Perfusion-weighted magnetic resonance imaging to distinguish the recurrence of metastatic brain tumors from radiation necrosis after stereotactic radiosurgery. J Neurooncol 2010;99(1):81—8.

[69] Barajas RF, Chang JS, Sneed PK, Segal MR, McDermott MW, Cha S. Distinguishing recurrent intra-axial metastatic tumor from radiation necrosis following gamma knife radiosurgery using dynamic susceptibility-weighted contrast-enhanced perfusion MR imaging. AJNR Am J Neuroradiol 2009;30(2):367—72.

[70] Chernov MF, Hayashi M, Izawa M, Usukura M, Yoshida S, Ono Y, et al. Multivoxel proton MRS for differentiation of radiation-induced necrosis and tumor recurrence after gamma knife radiosurgery for brain metastases. Brain Tumor Pathol 2006;23(1):19—27.

[71] Chao ST, Suh JH, Raja S, Lee S-Y, Barnett G. The sensitivity and specificity of FDG-PET in distinguishing recurrent brain tumor from radionecrosis in patients treated with stereotactic radiosurgery. Int J Cancer 2001;96(3):191—7.

[72] Caroline I, Rosenthal MA. Imaging modalities in high-grade gliomas: pseudoprogression, recurrence, or necrosis? J Clin Neurosci 2012;19(5):633—7.

[73] Galldiks N, Stoffels G, Filss CP, Piroth MD, Sabel M, Ruge MI, et al. Role of O-(2-(18)F-fluoroethyl)-L-tyrosine PET for differentiation of local recurrent brain metastasis from radiation necrosis. J Nucl Med 2012;53(9):1367—74.

[74] Serizawa T, Saeki N, Higuchi Y, Ono J, Matsuda S, Sato M, et al. Diagnostic value of thallium-201 chloride single-photon emission computerized tomography in differentiating tumor recurrence from radiation injury after gamma knife surgery for metastatic brain tumors. J Neurosurg 2005;102Suppl:266—71.

[75] Kickingereder P, Dorn F, Blau T, Schmidt M, Kocher M, Galldiks N, et al. Differentiation of local tumor recurrence from radiation-induced changes after stereotactic radiosurgery for treatment of brain metastasis: case report and review of the literature. Radiat Oncol 2013;8:52.

[76] Kohshi K, Imada H, Nomoto S, Yamaguchi R, Abe H, Yamamoto H. Successful treatment of radiation-induced brain necrosis by hyperbaric oxygen therapy. J Neurol Sci 2003;209(1—2):115—7.

[77] Boothe D, Young R, Yamada Y, Prager A, Chan T, Beal K. Bevacizumab as a treatment for radiation necrosis of brain metastases post stereotactic radiosurgery. Neuro Oncol 2013;15(9):1257—63.

[78] Sadraei NH, Dahiya S, Chao ST, Murphy ES, Osei-Boateng K, Xie H, et al. Treatment of cerebral radiation necrosis with bevacizumab: the cleveland clinic experience. Am J Clin Oncol 2013 [Epub ahead of print].

[79] Levin VA, Bidaut L, Hou P, Kumar AJ, Wefel JS, Bekele BN, et al. Randomized double-blind placebo-controlled trial of bevacizumab therapy for radiation necrosis of the central nervous system. Int J Radiat Oncol Biol Phys 2011;79(5):1487—95.

[80] Chao ST, Ahluwalia MS, Barnett GH, Stevens GHJ, Murphy ES, Stockham AL, et al. Challenges with the diagnosis and treatment of cerebral radiation necrosis. Int J Radiat Oncol Biol Phys 2013;87(3):449—57.

[81] Telera S, Fabi A, Pace A, Vidiri A, Anelli V, Carapella CM, et al. Radionecrosis induced by stereotactic radiosurgery of brain metastases: results of surgery and outcome of disease. J Neurooncol 2013;113(2):313—25.